Corneal Collagen Cross-Linking Pretreatment Mitigates Injury-Induced Inflammation, Hemangiogenesis and Lymphangiogenesis In Vivo

Yirui Zhu[1,2], Peter S. Reinach[1], Chaoxiang Ge[1], Yun Li[1], Biao Wu[1], Qi Xie[1], Louis Tong[3–6], and Wei Chen[1]

[1] School of Ophthalmology and Optometry and Eye Hospital, Wenzhou Medical University, Zhejiang, China
[2] Eye Center of the 2nd Affiliated Hospital, Medical College of Zhejiang University, Hangzhou, Zhejiang, China
[3] Yong Loo Lin School of Medicine, National University of Singapore, Singapore, Singapore
[4] Singapore National Eye Centre, Singapore, Singapore
[5] Singapore Eye Research Institute, Singapore, Singapore
[6] Duke-NUS Medical School, Singapore, Singapore

Correspondence: Wei Chen, The School of Ophthalmology and Optometry and Eye Hospital, Wenzhou Medical University, 270 Xueyuan West Road, Wenzhou, Zhejiang 325027, People's Republic of China.
e-mail: chenweimd@wmu.edu.cn
Louis Tong, Singapore National Eye Center, 11 Third Hospital Avenue, Singapore 168751, Singapore.
e-mail: louis.tong.h.t@singhealth.com.sg

Purpose: The purpose of this study was to evaluate if corneal collagen cross-linking (CXL) pretreatment dampens suture-induced hemangiogenesis and lymphangiogenesis driven by inflammation.

Methods: Four weeks after CXL pretreatment, suture emplacement was performed in rats. The time dependent effects were compared of this procedure in three groups: (1) suture-induced neovascularization (SNV group); (2) CXL treatment prior to suture-induced neovascularization (CXL + SNV group); (3) Normal control (NC group). Serial morphometric measurements evaluated suture-induced hemangiogenesis and lymphangiogenesis. CD45 and CD68 immunofluorescent staining pattern changes determined immune cell activation, stromal leucocyte, and macrophage infiltration. The real-time quantitative polymerase chain reaction (RT-qPCR) determined angiogenic and lymphangiogenic gene expression level changes. Western blots evaluated protein expression levels of vascular endothelial cell CD31 and lymphatic vessel endothelial hyaluronan receptor (LYVE-1).

Results: On days 7 and 14 after suture emplacement, the rises in angiogenesis, lymphangiogenesis, CD45+ and CD68+ cell infiltration were less in the CXL pretreated (CXL + SNV) group than in the untreated (SNV) group. Angiogenic and lymphangiogenic mRNA levels and CD31 and LYVE-1 protein and proinflammatory cytokines were also suppressed, confirming that CXL pretreatment improved the wound healing response.

Conclusions: CXL pretreatment inhibits injury-induced angiogenesis and lymphangiogenesis. These reductions suggest that prior CXL therapy decrease ocular inflammation reactivated by secondary trauma.

Translational Relevance: CXL pretreatment induces increases in stromal stiffness which in turn reduces trauma or microbial driven increases in inflammation, angiogenesis, and lymphangiogenesis. These beneficial effects suggest that this novel procedure may improve therapeutic management of trauma-induced corneal disease in a clinical setting.

Introduction

Corneal collagen cross-linking (CXL) is a noninvasive technique that combines ultraviolet A radiation and riboflavin to stiffen corneal tissue through collagen fiber photopolymerization.[1] An increasing number of clinical studies suggest that this procedure is both safe and effective in slowing down or even halting the progression of keratoconus.[2–4]

translational vision science & technology

Some biochemical and biophysical measurements demonstrated that CXL enhances both corneal rigidity and biomechanical stability.[5,6] Although slight increases in aqueous flare following various CXL procedures with keratoconus were previously reported, the CXL procedure in that scenario did not induce significant postoperative inflammation.[7] As CXL is becoming widely used to strengthen corneal tissue in ectatic disorders, it is necessary to investigate whether or not the CXL-induced tissue modifications also affect inflammatory-induced angiogenesis and lymphangiogenesis following trauma or microbial infection. Our previous study shows that CXL treatment increases the anterior stromal collagenous architectural compaction with keratocyte apoptotic changes.[8]

We recently established a novel rat high-intensity CXL model that characterizes corneal inflammatory responses induced by riboflavin and UVA exposure. Our results suggest that the CXL procedure is safe because 4 weeks post CXL, the inflammatory index and corneal thickness were similar to those in untreated corneas.[8] However, because the CXL was performed shortly (3 days) after suture placement, we were unable to determine if the modulatory effect of CXL was due to mechanical factors rather than activation of interacting inflammatory signaling pathways. To distinguish between these possibilities, we performed a study which used CXL pretreatment followed by a time delay to await resolution of inflammation before performing suture emplacement. The outcome of interest was to evaluate the magnitudes of hemangiogenesis, and lymphangiogenesis, as well as their underlying mechanisms. In the long term, this assessment is an important first step toward developing a nonpharmacological method to reduce corneal angiogenesis, an important sight-threatening condition that often lacks restorative therapy.[9]

Materials and Methods

Study Design

This study was approved by the Animal Care and Ethics Committee of Wenzhou Medical University, Wenzhou, China, and adhered to the (ARVO) Statement for the Use of Animals in Ophthalmic and Vision Research. A total of 183 Sprague-Dawley rats (8 to 10 weeks old) were randomly divided into two different studies. Rats were randomized into 3 groups: (1) The suture-induced neovascularization (SNV) group ($n = 75$) received a suture with a 10-0 thread emplacement in the right eye; (2) The CXL + SNV group ($n = 75$) received CXL pretreatment of 9 mW/cm^2 UVA
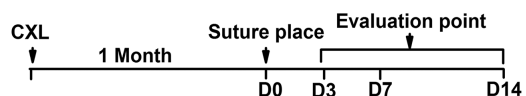
Figure 1. Schedule for evaluating if CXL pretreatment reduces responses to suture emplacement in rat corneas.

exposure for 240 seconds and 0.22% topical riboflavin eyedrops. Four weeks later, a suture was emplaced in the right eye; (3) both eyes of the normal control (NC group, $n = 33$) were left untreated and unsutured. The eyes of the 3 groups were evaluated 3, 7, and 14 days after suture emplacement (Fig. 1).

Suture-Induced Neovascularization

Prior to suture emplacement, animals were deeply anesthetized by intraperitoneal injection of ketamine (50–75 mg/kg) and xylazine (5 mg/kg). Anesthetic eye drops composed of 0.5% proparacaine hydrochloride (Alcaine; Alcon, Inc., Fort Worth, TX, USA) were applied to the right eye. Three single sutures (10-0) were sown through the peripheral stroma approximately 1.5 to 2 mm removed from the temporal limbus at the 4, 8, and 12 o'clock positions in 2 groups. Sutures were left in place for 14 days.

Neovascularization Assay

Neovascularization was evaluated at 3, 7, and 14 days after suture emplacement using a slightly modified method described elsewhere.[10] Briefly, three photographs of each cornea were taken using a digital camera (EOS 5200D; Canon, Tokyo, Japan) under green light at 16 times magnification (10 corneas per group); 360 degree area of corneal new vessels was analyzed at the same magnification using ImageJ software. The area between the innermost new vessel and the limbus was defined as the vascularized area. The degree of neovascularization was determined by dividing the vascularized area by the total corneal area (measured in pixels). Vessel density values were then computed from a binarized image as a ratio of the area of the white pixels (vessels) to the whole image pixel area using ImageJ. Photographs were analyzed in a random order by two double-blinded investigators to minimize observer bias.

Morphometry of Lymphangiogenesis

After taking photographs under a slit lamp, 5 rats in each group were euthanized on days 3, 7, and 14 following suture emplacements. Eyes from freshly euthanized rats were enucleated and

Table. Rat Primer Sequences Used for Real-Time qPCR

Gene	Sense Primer	Antisense Primer
GAPDH	TCTCTGCTCCTCCCTGTTC	ACACCGACCTTCACCATCT
CD31	TGGTGCTTCGGTGCTCTGTGA	GCTGGCTCTGTTGAACGCTGTA
Vascular cell adhesion molecule-1 (VCAM-1)	GCTGCTGTTGGCTGTGACTCTC	GGCTCAGCGTCAGTGTGGATGT
Vascular endothelial growth factor receptor 2 (VEGFR2)	CCTGTATGGAGGAAGAGGAAGTGT	TGTCTGGCTGTCATCTGGAATCA
Vascular endothelial growth factor receptor 3 (VEGFR3)	ACCTCTCCAACTTCTTGCGTGTCA	GGTGCTTCCAAGTCTCCTCCTATCA
Vascular endothelial growth factor C (VEGFC)	TCTTGTCTCTGGCGTGTTCCTT	CACAGACCGCAACTGCTCCT
LYVE-1	CCAGCAGGAACCAGGTGGAATC	AGGTGTCAGATGAGTTGTGGCAAT
TNF-α	GCCCAGACCCTCACACTCAGAT	TGCTCCTCCGCTTGGTGGTT
IFN-γ	TGAACAACCCACAGATCCAGCACAA	CCCAGAATCAGCACCGACTCCTTT
MMP-9	CCACCACCGCCAACTATGACCA	TGCTTGCCCAGGAAGACGAAGG
MCP-1	CCACTCACCTGCTGCTACTCATTCA	GCTTCTTTGGGACACCTGCTGCT

placed into corneal flat mounts. For whole-mount staining, freshly excised corneas were washed in phosphate-buffered saline (PBS) and fixed in acetone for 15 minutes. Specimens were immunostained with rabbit anti-mouse lymphatic vessel endothelial hyaluronan receptor (LYVE-1) antibody (1:100; sc-28190; Santa Cruz Biotechnology, Inc.) overnight at 4°C, washed with PBS, incubated with secondary goat anti-rabbit antibody (1:100; Abcam), and mounted with Vector Shield mounting medium (Vector Laboratories, Burlingame, CA, USA). Corneas were analyzed using a confocal microscope (LSM710; Zeiss with krypton-argon and He-Ne laser; Carl Zeiss Meditec, Sartrouville, Germany). ImageJ software determined the area and density covered by angiogenesis and lymphatic vessels.

Immunofluorescent Staining

Five corneas from different rats in each group were excised posttreatment. Sections were fixed with methanol at 4°C for 10 minutes, washed with PBS for 15 minutes, blocked with 20% normal goat serum solution for 1 hour, and incubated with mouse monoclonal antibody anti-CD45 (ab33984; Abcam, Cambridge, MA, USA; 1:200), anti-CD68 (ab125212; Abcam, Cambridge, MA, USA; 1:200) at 4°C overnight. Following incubation with goat anti-mouse Alexa Fluor 488-conjugated secondary antibody (ab96879; Abcam; 1:300), the sections were washed in 0.01 M PBS, 4′6-diamidino-2-phenylindole (DAPI; Invitrogen, Carlsbad, CA, USA; 1:1000) and then stained for 5 minutes. After sealing, sections were photographed with the aforementioned laser scanning confocal microscope at 200 times magnification. As previously described, the immunostained cells were counted in five non-overlapping areas (0.1 mm × 0.1

mm) in three separate corneal sections extending across the entire stroma.[11,12]

Real-Time PCR

Total RNA was extracted from two corneas (RNeasy mini kit [50×], Qiagen, Crawley, UK). DNAase treatment eliminated genomic DNA contamination. RNA was reverse transcribed with M-MLV reverse transcriptase according to the manufacturer's instructions (Promega, Madison, WI, USA). The primers were designed using Primer Express 3.0 software (Applied Biosystems Inc., Foster City, CA, USA), and their sequences are provided in the Table. PCRs were performed using a 7500 Real-Time PCR System (Applied Biosystems) with the Power SYBR Green PCR Master Mix (Applied Biosystems, Paisley, UK). The mRNA expression levels were analyzed by the comparative threshold cycle (Ct) method and normalized to the housekeeping gene GAPDH expression level.

Western Blotting

Western blot analysis evaluated angiogenesis and lymphangiogenesis based on protein expression levels of CD31 and LYVE-1 as respective biomarkers on days 3, 7, and 14 post suture emplacements, respectively. From each group of 9 pooled corneas, proteins were extracted with cold RIPA buffer and subjected to electrophoresis on 10% sodium dodecyl sulfate-polyacrylamide gels according to a previously described protocol.[13] Membranes were blocked with fat-free milk and then probed overnight with primary antibodies (CD31, LYVE-1, and GAPDH, 1: 500) and secondary antibodies (HRP-conjugated goat anti-rabbit IgG; Santa Cruz Biotechnology, Santa Cruz, CA, USA; 1: 2500). The specific bands were visualized

by an enhanced chemiluminescence reagent (Pierce Biotechnology, Inc., Rockford, IL, USA), and each resolvable band was normalized to the corresponding GAPDH expression level.

Statistical Analysis

The Mann-Whitney U test, the Kruskal-Wallis test, and one-way ANOVA were performed for multiple comparisons among groups, and SPSS 19.0 (SPSS; IBM Corporation, Chicago, IL, USA) was used for all analyses. A value of $P < 0.05$ was considered statistically significant.

Results

CXL Pretreatment Suppresses Suture-Induced Hemangiogenesis and Lymphangiogenesis

To determine if CXL pretreatment affects suture emplacement induced neovascularization, its effects were determined by comparing vascularized areas in the CXL + SNV with those in the SNV groups on days 3, 7, and 14. The images shown in Figure 2 indicate that on day 3 after suture emplacement neovascularization was the same in both groups. On the other hand, on days 7 and 14, neovascularization in the CXL + SNV group was significantly less than that in the SNV group ($P < 0.01$; see Figs. 2A–F). In the SNV corneas, it was 73.8 ± 4.9% on day 7 and 87.2 ± 6.5% on day 14, respectively. In contrast, the vascularized area of the CXL + SNV corneas was 53.3 ± 5.6% on day 7 and 69.9 ± 5.9% on day 14, respectively (Fig. 2G). The vascularized density of the SNV corneas was 60.5 ± 5.3% on day 7 and 70.1 ± 4.6% on day 14. In the CXL + SNV corneas, it was 44.9 ± 4.5% on day 7 and

52.6 ± 6.2% on day 14, respectively (Fig. 2H). Therefore, CXL pretreatment reduced suture emplacement-induced neovascularization.

CXL pretreatment and suture emplacement effects on lymphangiogenesis were evaluated based on endothelial hyaluronan receptor-1 immunostaining pattern changes on infiltrating lymphatic vessels in corneal flat mounts. In the CXL + SNV treated corneas on days 7 and 14, this response was less than that in the SNV corneas ($P < 0.01$; Figs. 3A–F). The lymphatic coverage areas in the SNV corneas were 68.6 ± 4.9% on day 7 and 90.4 ± 9.1% on day 14, respectively. In contrast, in the CXL + SNV corneas, they were 43.6 ± 4.0% on day 7 and 75.0 ± 8.3% on day 14, respectively (Fig. 3G). The lymphatic coverage density of the SNV corneas was 45.7 ± 3.2% on day 7 and 57.3 ± 6.1% on day 14. In the CXL + SNV corneas, it was 27.1 ± 2.6% on day 7 and 42 ± 3.5% on day 14, respectively (Fig. 3H). Therefore, CXL pretreatment also inhibited suture emplacement induced lymphangiogenesis.

### CXL Pretreatment Decreased Inflammatory Cell Infiltration

CXL pretreatment reduced suture emplacement induced increases in CD45+ leukocyte and CD68+ macrophage immunostaining and infiltration, respectively (Figs. 4A–I; Figs. 5A–I). In the NC group, their immunostaining patterns were almost exclusively limited to the peripheral cornea and the limbus. On days 3, 7, and 14 after suture emplacement, CD45 and CD68 expression levels in this region were significantly less in the CXL + SNV-treated group than in the SNV group ($P < 0.05$, $P < 0.01$, respectively; Fig. 4J, Fig. 5J). These lower levels are indicative of fewer leukocytes and macrophages in the CXL + SNV-treated corneas than in their SNV counterpart.
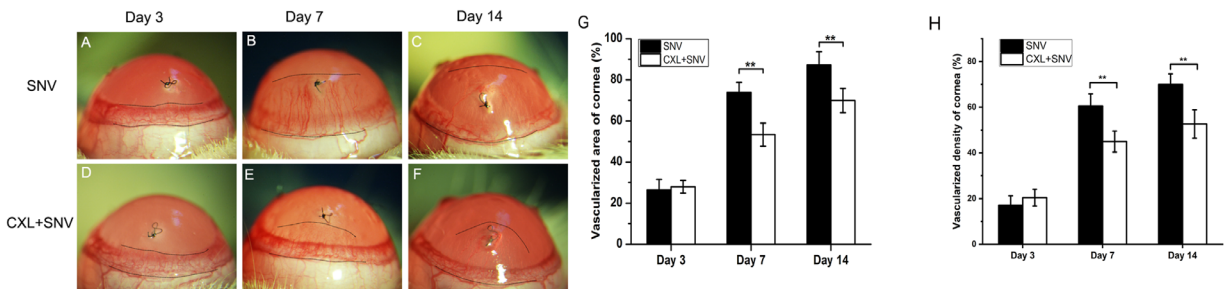
Figure 2. CXL pretreatment suppresses subsequent suture emplacement-induced hemangiogenesis. (**A–F**) Suture-induced corneal neovascularization in CXL-treated corneas. Typical images of SNV and CXL + SNV groups on days 3 to 14 after suture emplacement. (**G, H**) CXL-treatment reduced blood vessel proliferation compared with that in the SNV group (*******P* < 0.01) in vivo on days 7 and 14 post suture. Original magnification, time 16.
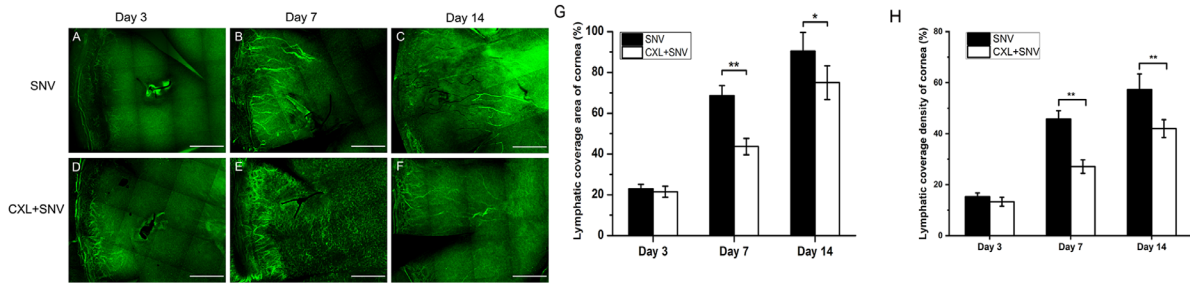
Figure 3. Summary of time dependent increases in lymphangiogenesis based on rises in LYVE-1 immunostaining. (**A–F**) Representative images of corneal LYVE-1 immunostained flat-mounted corneas 3, 7, and 14 days after suture emplacement. (**G, H**) Lymphangiogenesis decreased in the CXL + SNV cornea compared with that in the SNV corneas (data are shown as mean ± SEM, $n = 6$, *$P < 0.05$, **$P < 0.01$). Original magnification, times 100.
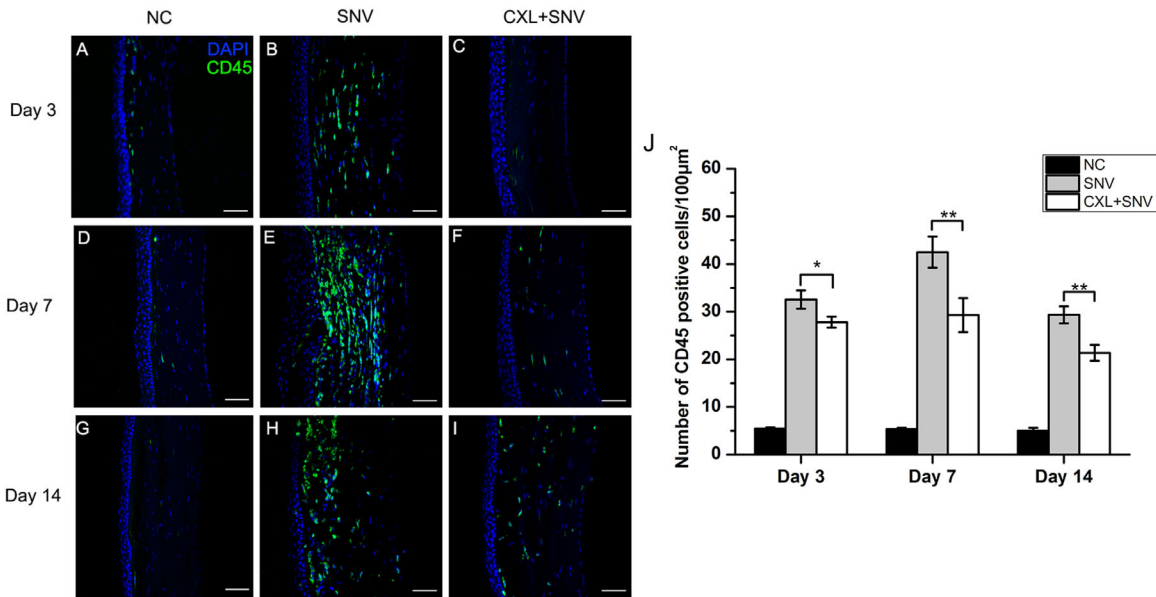
Figure 4. CXL pretreatment suppresses subsequent suture emplacement-induced activated immune cell infiltration. (**A–I**) In CXL-treated corneas, suture emplacement induced less CD45 marked leukocyte infiltration (green) than in untreated sutured corneas on days 3, 7, and 14. Stromal CD45 immunostaining analysis in NC, SNV corneas, and CXL + SNV corneas. (**J**) Quantification of CD45 stained infiltrating leukocytes per field. CXL pretreatment reduced suture induced leukocyte infiltration relative to that in SNV treated corneas on days 3, 7, and 14 (*$P < 0.05$, **$P < 0.01$ versus SNV group; data are shown as mean ± SEM).

CXL Pretreatment Suppresses Increases in Proangiogenic, Prolymphangiogenic, and Proinflammatory Cytokine Gene Expression Levels

To confirm that CXL pretreatment reduced corneal hem- and lymphangiogenesis, real-time PCR analysis assessed its effects on CD31, VCAM-1, VEGFR2, VEGFR3, VEGFC, and LYVE-1. On days 3, 7, and 14 following suture emplacements, all of these mRNA expression levels in the CXL + SNV corneas were significantly downregulated compared to those in the SNV group ($P < 0.05$, $P < 0.01$, respectively; Figs. 6A–F). These differences between the CXL + SNV

and the SNV groups validate that CXL pretreatment inhibited corneal angiogenesis and lymphangiogenesis. On days 7 and 14 post suture emplacement, IFN-γ, TNF-α, and MCP-1 mRNA expression levels were significantly lower in the CXL + SNV than those in the SNV group ($P < 0.01$; Figs. 6G–J).

CXL Pretreatment Suppresses Suture Emplacement-induced CD31 and LYVE-1 Protein Expression Level Transients

CD31 and LYVE-1 baseline protein expression levels were low in the NC group whereas they increased
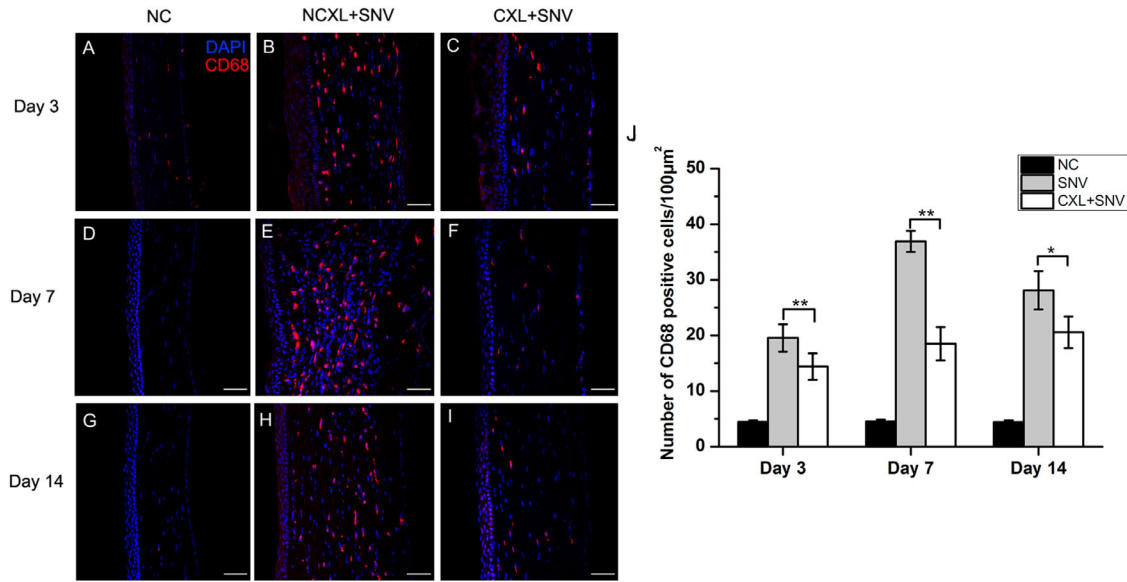
Figure 5. (**A–I**) CD68 marked macrophage infiltration (red) induced by a corneal suture was inhibited in CXL-treated corneas on days 3, 7, and 14. CD68 stromal immunostaining analysis in NC, SNV, and CXL + SNV groups. (**J**) Quantification of infiltrating CD68 macrophages per field. CD68 positive macrophage infiltration was significantly greater in SNV than CXL + SNV corneas at days 3, 7, and 14 (*$P < 0.05$, **$P < 0.01$ versus SNV group; data are shown as mean ± SEM).
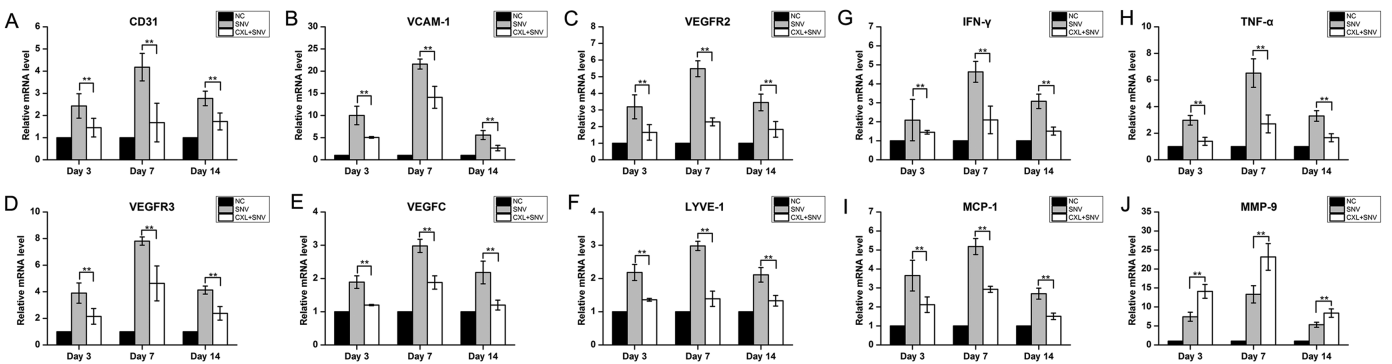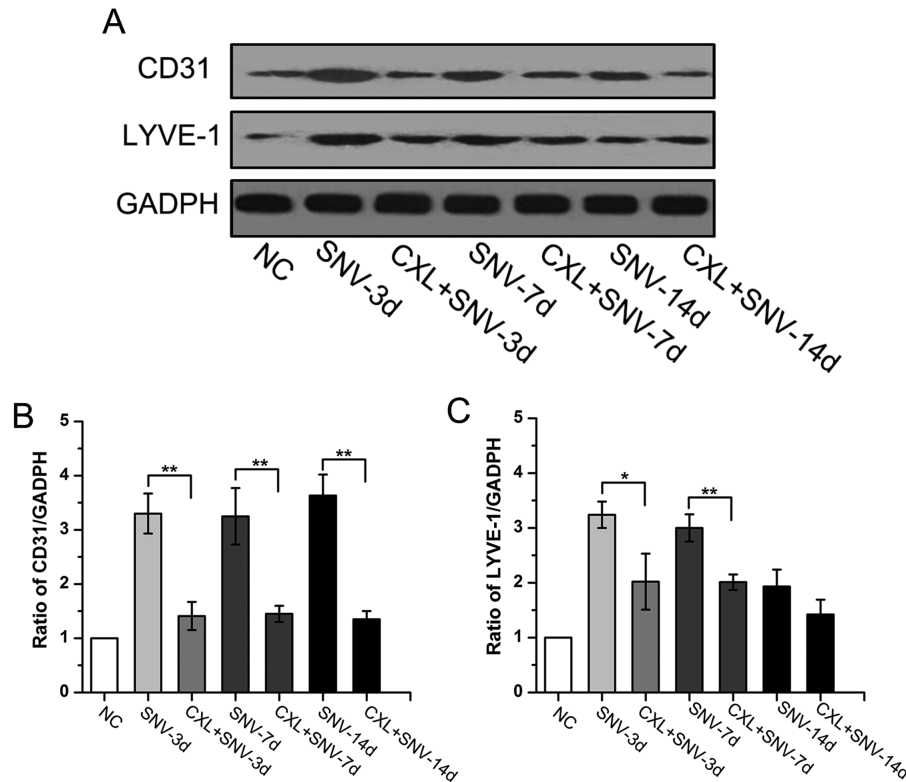

Figure 6. (**A–F**) CXL pretreatment suppresses subsequent suture emplacement induced increases in hemangiogenic and lymphangiogenic gene expression levels. Quantitative real-time PCR results show significant declines in CD31, VCAM-1, VEGFR2, VEGFR3, VEGFC, and LYVE-1 in the CXL + SNV corneas on days 3, 7, and 14 post suture. (**G–J**) CXL pretreatment suppresses subsequent suture emplacement induced increases in proinflammatory gene expression levels. Significant decreases in IFN-γ, TNF-α, and MCP-1 on days 3, 7, and 14 post suture, whereas MMP-9 expression levels increased in the CXL + SNV corneas.

considerably after suture emplacement in the SNV group. On the other hand, these rises were less in the CXL + SNV group than in the SNV group on days 3, 7, and 14 ($P < 0.05$, $P < 0.01$, respectively; Fig. 7). These smaller increases indicate that this procedure inhibited suture emplacement-induced lymphangiogenesis, which was accompanied by less vascular endothelial cell tube elongation.

Discussion

We now provide clear evidence that prior CXL and time delay between performing the CXL procedure and suture emplacement reduced the magnitude and delayed subsequent lymphogenesis and hemangiogenesis compared to suture alone. In our previous study,

translational vision science & technology

Figure 7. (**A**) CXL pretreatment suppresses suture induced increases in CD31 and LYVE-1 protein expression levels. (**B, C**) A significant decrease in CD31 and LYVE-1 protein expression levels was observed in the CXL + SNV group relative to those in the SNV group on days 3, 7, and 14 (*$P < 0.05$, **$P < 0.01$, respectively).

suture emplacement instead preceded CXL treatment, which occurred 3 days later. After waiting another 4 days, the induced increases in hemangiogenesis and lymphogenesis were less than those in the untreated control corneas. However, these declines mediated by CXL were only transient because by day 14 they had fully reversed back to the elevated levels that were reached immediately following CXL. Underlying this time course of transient changes, proinflammatory TNF-α, IFN-γ, MCP-1, and MMP-9 cytokines and VEGFs expression levels showed similar trends. However, in the current study, CXL pretreatment suppressed the rises in lymphogenesis and hemangiogenesis for a longer period compared to this previous study. This delay occurred because we have temporally separated from one another performance of the CXL and the suture emplacement procedures. CXL by itself increases immune cell corneal infiltration, but this inflammation is resolved after 28 days. Therefore, a pretreatment period of 28 days is needed to resolve the benefit of CXL that is not offset by acute CXL-induced increases in inflammatory processes.

The cornea is one of the lymphangiogenic and hemangiogenic privileged sites in the human body. When its avascular system is disrupted by any type of intervention, such as trauma, infection, conjunctival derived blood, and lymphatic vessels can easily infiltrate into the corneal surface. Blood and lymphatic vessels in the cornea play important roles in mediating the immune responses induced by corneal infection transplantation.[14] Thus, anti(lymph) angiogenic therapy has emerged as a potential strategy to improve graft survival after keratoplasty.

There is substantive evidence that CXL is an effective procedure for treating corneal neovascularization in a clinical setting based on its direct suppression of vascular endothelial elongation, immune cell proliferation, and infiltration.[15] In some clinical cases, peripheral CXL was used to regress targeting pre-existing pathological corneal blood and lymphatic vessels before or during performing penetrating keratoplasty.[16] These studies revealed that CXL treatment similarly targets both corneal blood and lymphatic vessel extension.

Although there are several available CXL strategies to inhibit pre-existing corneal neovascularization, the current study work focused on evaluating the effect of CXL pretreatment by itself on inducing changes in lymphogenesis and hemangiogenesis. Both of these injury-induced responses were

significantly suppressed in the CXL + SNV group on days 7 and 14 compared to the rises in the SNV group. Furthermore, CXL pretreatment reduced the subsequent increases in the infiltration of CD45-labeled leucocytes and CD68-labeled macrophages induced by suture emplacement. One possible explanation for how CXL pretreatment suppressed these responses is that this procedure altered structural stromal integrity and increased corneal stiffness. These changes could hinder endothelial cell tube formation, extension, and lymphatic vessel infiltration. Injury-induced macrophage infiltration plays a key role in mediating factors that promote angiogenesis and lymphangiogenesis.[17–19] Another possible explanation of our previous study[20] is that the CXL-induced inflammation can somehow compete or interfere with the suture induced inflammation. However, this alternative is excluded because of our current strategy of waiting for CXL inflammation to be resolved before performing suture emplacement.

Some or all of these differences related to CXL pretreatment could be associated with increases in extracellular matrix (ECM) density because in vivo confocal microscopy showed that ECM density remained higher even 3 years after keratoconus patients had received CXL pretreatment.[21] Our previous study also indicates that compacted collagenous architecture possibly obstructs inflammatory cell infiltration.[10] However, the mechanism remains unknown that accounts for how a more compacted ECM impedes immune infiltration.

Extracellular matrix (ECM) stiffness, apart from determining corneal biomechanical strength, can also alter fibroblast behavior.[22,23] ECM stiffness is well recognized as an independent regulator of cell migration, proliferation, and stem cell differentiation.[24,25] In the ECM, the relative proportions of the collagen subtypes and their physical and chemical properties regulate deformability of large veins and arteries.[26] In addition, patency of small caliber vessels, such as retinal venules, depends on properties of the basement membrane and the subendothelial matrix.[27] In the cornea, the ECM makeup modulates the communication between the endothelial cells and the surrounding tissue. During sprouting of new vessels, the ECM is proteolytically altered and unable to inhibit further angiogenesis.[28,29] Therefore, CXL could alter ECM components to stiffen the matrix, and inhibit the migratory and sprouting behavior of vascular and lymphatic endothelial cells.

Among all the different angiogenic and lymphogenic factors, different VEGF species play pivotal roles in mediating these responses. During angiogenesis, an increase in VEGFR2 expression contributes to rises in proliferation and internalization of vascular endothelial cells to cause elongation of nascent blood vessels.[30] On the other hand, VEGFR3 binding with VEGFC stimulates the development of lymphatic vessels. VEGFR2 upregulation was reported along with stimulation of capillary blood vessel formation in a soft microenvironment. As with VEGFR2, VEGFR3 also underwent upregulation, which may have occurred as a consequence of a decrease in matrix stiffness. This effect may also account for increases in lymphatic endothelial cell infiltration and migration.[31] These findings are consistent with our real-time quantitative polymerase chain reaction (RT-qPCR) results showing changes in VEGFR2, VEGFC, and VEGFR3 expression levels.

It is now well established that immune cell activation is a mechanosensitive process. The cytoskeletal architecture of leukocytes can undergo complete reorganization. Their migratory and communicative functions can exert substantial mechanical force to reduce ECM stiffness.[32] Cell-matrix interactions involve stronger contractile forces on stiffer surfaces than on more compliant ones.[33,34] It is possible that robust signaling associated with stiffer substrates triggers activation-induced cell death, which could prevent lymphocyte expansion.[35,36] These results may explain the CXL-induced inhibition of immune cell activation and infiltration.

In conclusion, we used a novel high-intensity CXL rat model supplemented with riboflavin to show that CXL pretreatment reduced the subsequent immune cell activation and infiltration that underlies inflammation induced by suture emplacement. Such inhibition is consistent with the observed declines in hemangiogenesis and lymphangiogenesis. These reductions suggest that prior CXL therapy may be beneficial to prevent the adverse complications of trauma-induced corneal disease. Further studies are required to determine if CXL pretreatment improves the outcome of specific types of traumas in clinical scenarios, such as corneal keratoplasty.

Acknowledgments

Author Contributions: Y.Z. and W.C. conceived and designed the experiments. Y.Z., C.G., and Y.L. executed the animal surgery and observation. Y.Z., C.G., Y.L., B.W., and Q.X. contributed to the PCR, staining, and

References

1. Randleman JB, Khandelwal SS, Hafezi F. Corneal cross-linking. *Surv Ophthalmol*. 2015;60:509–523.

2. Wollensak G, Spoerl E, Seiler T. Riboflavin/ultraviolet-a–induced collagen crosslinking for the treatment of keratoconus. *Am J Ophthalmol*. 2003;135:620–627.

3. Spoerl E, Mrochen M, Sliney D, Trokel S, Seiler T. Safety of UVA-riboflavin cross-linking of the cornea. *Cornea*. 2007;26:385–389.

4. Wittig-Silva C, Chan E, Islam FM, Wu T, Whiting M, Snibson GR. A randomized, controlled trial of corneal collagen cross-linking in progressive keratoconus: three-year results. *Ophthalmology*. 2014;121:812–821.

5. Hammer A, Richoz O, Arba Mosquera S, Tabibian D, Hoogewoud F, Hafezi F. Corneal biomechanical properties at different corneal cross-linking (CXL) irradiances. *Invest Ophthalmol Vis Sci*. 2014;55:2881–2884.

6. Richoz O, Hammer A, Tabibian D, Gatzioufas Z, Hafezi F. The Biomechanical Effect of Corneal Collagen Cross-Linking (CXL) With Riboflavin and UV-A is Oxygen Dependent. *Transl Vis Sci Technol*. 2013;2:6.

7. Hedayatfar A, Hashemi H, Aghaei H, Ashraf N, Asgari S. Subclinical Inflammatory Response: Accelerated versus Standard Corneal Cross-Linking. *Ocul Immunol Inflamm*. 2019;27:513–516.

8. Zhu Y, Reinach PS, Zhu H, et al. High-intensity corneal collagen crosslinking with riboflavin and UVA in rat cornea. *PLoS One*. 2017;12:e0179580.

9. Roshandel D, Eslani M, Baradaran-Rafii A, et al. Current and emerging therapies for corneal neovascularization. *Ocul Surf*. 2018;16:398–414.

10. Zhu Y, Li L, Reinach PS, et al. Corneal Collagen Cross-Linking With Riboflavin and UVA Regulates Hemangiogenesis and Lymphangiogenesis in Rats. *Invest Ophthalmol Vis Sci*. 2018;59:3702–3712.

11. Han SB, Ang H, Balehosur D, et al. A mouse model of corneal endothelial decompensation using cryoinjury. *Mol Vis*. 2013;19:1222–1230.

12. Chen W, Zhang X, Li J, et al. Efficacy of osmoprotectants on prevention and treatment of murine dry eye. *Invest Ophthalmol Vis Sci*. 2013;54:6287–6297.

13. Han Y, Shao Y, Lin Z, et al. Netrin-1 simultaneously suppresses corneal inflammation and neovascularization. *Invest Ophthalmol Vis Sci*. 2012;53:1285–1295.

14. Hori J, Yamaguchi T, Keino H, Hamrah P, Maruyama K. Immune privilege in corneal transplantation. *Prog Retin Eye Res*. 2019;72:100758.

15. Hou Y, Le VNH, Toth G, et al. UV light crosslinking regresses mature corneal blood and lymphatic vessels and promotes subsequent high-risk corneal transplant survival. *Am J Transplant*. 2018;18:2873–2884.

16. Schaub F, Hou Y, Zhang W, Bock F, Hos D, Cursiefen C. Corneal Crosslinking to Regress Pathologic Corneal Neovascularization Before High-Risk Keratoplasty. *Cornea*. 2021;40:147–155.

17. Kerjaschki D, Huttary N, Raab I, et al. Lymphatic endothelial progenitor cells contribute to de novo lymphangiogenesis in human renal transplants. *Nat Med*. 2006;12:230–234.

18. Kataru RP, Jung K, Jang C, et al. Critical role of CD11b+ macrophages and VEGF in inflammatory lymphangiogenesis, antigen clearance, and inflammation resolution. *Blood*. 2009;113:5650–5659.

19. Maruyama K, Asai J, Ii M, Thorne T, Losordo DW, D'Amore PA. Decreased macrophage number and activation lead to reduced lymphatic vessel formation and contribute to impaired diabetic wound healing. *Am J Pathol*. 2007;170:1178–1191.

20. Cagini C, Messina M, Torroni G, Riccitelli F, Mariniello M, Dua HS. Efficacy of topical microemulsion of fatty acids of the omega-3 series on the sub-epithelial corneal nerves regeneration after epithelium-off corneal collagen cross-linking for keratoconus. *Int Ophthalmol*. 2020;40:205–212.

21. Goldich Y, Marcovich AL, Barkana Y, Avni I, Zadok D. Safety of corneal collagen cross-linking with UV-A and riboflavin in progressive keratoconus. *Cornea*. 2010;29:409–411.

22. Birukova AA, Tian X, Cokic I, Beckham Y, Gardel ML, Birukov KG. Endothelial barrier disruption and recovery is controlled by substrate stiffness. *Microvasc Res*. 2013;87:50–57.

23. Lampi MC, Reinhart-King CA. Targeting extracellular matrix stiffness to attenuate disease: From molecular mechanisms to clinical trials. *Sci Transl Med*. 2018;10:eaao0475.

24. Gkretsi V, Stylianopoulos T. Cell Adhesion and Matrix Stiffness: Coordinating Cancer Cell Invasion and Metastasis. *Front Oncol*. 2018;8:145.

25. Klein EA, Yin L, Kothapalli D, et al. Cell-cycle control by physiological matrix elasticity and in vivo tissue stiffening. *Curr Biol*. 2009;19:1511–1518.

26. Laurent S, Boutouyrie P, Lacolley P. Structural and genetic bases of arterial stiffness. *Hypertension*. 2005;45:1050–1055.

27. Chaqour B. Caught between a "Rho" and a hard place: are CCN1/CYR61 and CCN2/CTGF the arbiters of microvascular stiffness? *J Cell Commun Signal*. 2020;14:21–29.

28. Luttun A, Dewerchin M, Collen D, Carmeliet P. The role of proteinases in angiogenesis, heart development, restenosis, atherosclerosis, myocardial ischemia, and stroke: insights from genetic studies. *Curr Atheroscler Rep*. 2000;2:407–416.

29. Bajou K, Noel A, Gerard RD, et al. Absence of host plasminogen activator inhibitor 1 prevents cancer invasion and vascularization. *Nat Med*. 1998;4:923–928.

30. Simons M, Gordon E, Claesson-Welsh L. Mechanisms and regulation of endothelial VEGF receptor signalling. *Nat Rev Mol Cell Biol*. 2016;17:611–625.

31. Mammoto A, Connor KM, Mammoto T, et al. A mechanosensitive transcriptional mechanism that controls angiogenesis. *Nature*. 2009;457:1103–1108.

32. Huse M. Mechanical forces in the immune system. *Nat Rev Immunol*. 2017;17:679–690.

33. Hui KL, Balagopalan L, Samelson LE, Upadhyaya A. Cytoskeletal forces during signaling activation in Jurkat T-cells. *Mol Biol Cell*. 2015;26:685–695.

34. Elosegui-Artola A, Oria R, Chen Y, et al. Mechanical regulation of a molecular clutch defines force transmission and transduction in response to matrix rigidity. *Nat Cell Biol*. 2016;18:540–548.

35. Judokusumo E, Tabdanov E, Kumari S, Dustin ML, Kam LC. Mechanosensing in T lymphocyte activation. *Biophys J*. 2012;102:L5–L7.

36. O'Connor RS, Hao X, Shen K, et al. Substrate rigidity regulates human T cell activation and proliferation. *J Immunol*. 2012;189:1330–1339.

translational vision science & technology